

High Performance Positive Electrolyte with Potassium Diformate (KDF) Additive for Vanadium Redox Flow Batteries

Xiaoyan Wei¹, Gang Wang^{*2}, Feng Li², Jie Zhang², Jinwei Chen², Ruilin Wang^{*2}

¹ College of Chemistry, Sichuan University, China

² College of Materials Science and Engineering, Sichuan University, China

*E-mail: electrowg100@scu.edu.cn; rl.wang@scu.edu.cn

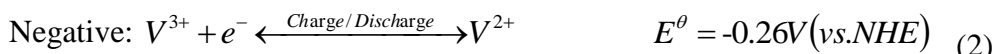
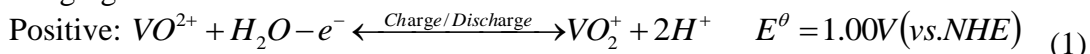
Received: 2 October 2021 / Accepted: 7 November 2021 / Published: 6 December 2021

Vanadium redox flow batteries (VRFB) are considered as one of the auspicious candidate for energy storage application. However, the low solubility and poor thermal stability of the positive electrolyte as technical bottlenecks restrict the application of VRFB. Here, we present potassium diformate (KDF) that could significantly improve the performance of the V(V) electrolyte. The precipitation time of the electrolyte with KDF has prolonged at high temperature compared with the pristine. The electrochemical activity of the electrolyte has been enhanced significantly, and the corresponding cycle stability of the battery is also remarkably increased. Results revealed that the energy efficiency of battery with V(V) electrolyte containing KDF is higher than that of the pristine during cycling tests.

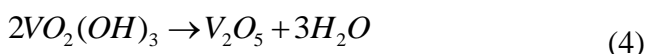
Keywords: VRFB; positive electrolyte; additive; potassium diformate

1. INTRODUCTION

The VRFB is a kind of large-scale energy storage battery system from kW to MW[1-5] and its main advantages are long life, simple structure, low maintenance cost and repeated use [6]. The charging and discharging reactions of VRFB are as follows:



VRFB system is composed of vanadium elements with different valence ions, the cross contamination of electrolyte caused by the ion diffusion across from the separator is avoided during the charging and discharging process[7]. However, the VO_2^+ ions of positive electrolyte show low solubility and are unstable at high temperature, which are easy to dehydrate and shrink to V_2O_5 precipitation. This precipitation process generally takes place in two steps, starting from the deprotonization of five coordinated V(V) ions[8] (Eq. (3), (4)):



The initial V_2O_5 nanoparticles can still be redissolved, but if the conditions of precipitation growth are met, these V_2O_5 nuclei will gradually grow into precipitates and are not easy to redissolve, which will eventually lead to rapid capacity attenuation and even blockage of the electrolyte flow system, thus decrease the battery efficiency. The most direct and effective way to improve the stability of VRFB positive electrolyte is to introduce efficient additives. At present, a lot of work has been done on the research of additives for the stability of positive electrolyte. Some inorganic additives, such as phosphate additives[6,9-16], can improve the thermal stability of V(V) electrolyte by forming a stable complex between P and V(V) and the common ion effect of cations, and inorganic acid[9,17] can improve the thermal stability of V(V) electrolyte by optimizing the acidity of the solution. In addition, organic compounds such as alcohols[18], acids[7,9] or salts[19] with special functional groups can inhibit the precipitation and improve the electrochemical activity of V(V) electrolyte due to the formation of intermediates. Other substances, such as dispersant[20], complexing agent[21], surfactant[7,22] and amino acid[23], with special structure, can also improve the thermal stability and electrochemical activity by preventing the agglomeration of V(V) ions and enhance the transfer of vanadium ions.

Taking sodium formate [24] as an example, studies show that sodium formate can improve the thermal stability of V(V) electrolyte by forming the hydrated penta coordinated vanadate ion structure. Metal-organic salts have the dual effects of organic functional groups and metal cations. Considering the promotion effect of carboxyl group on the positive electrolyte and the same ion effect of K^+ in the mixed electrolyte (the radius of K^+ is large, which is conducive to the dispersion of VO_2^+), three organic carboxylic potassium salts as additives were compared and the best one was selected and investigated.

2. EXPERIMENT

2.1 Determination of V(V) electrolyte and additives

V(V) electrolyte was prepared by electrolytic method [9], and V(V) concentration and solution acidity were determined by potentiometric titrator (916 Ti-Touch potentiometric titrator, Metrohm).

Table 1. Organic carboxylic potassium salts additives for V(V) electrolyte

Additive category	Name	Molecular structure
Organic carboxylic potassium salts	Potassium acetate (KAc)	
	Potassium diformate (KDF)	
	Potassium acrylate hydrate (KAH)	

The results showed that the V(V) concentration was 2.876 M, and the total hydrogen ions concentration was 12 M, so the electrolyte system was 2.876 M V(V) + 6 M H₂SO₄. Three organic carboxylic potassium salts additives have been used for V(V) electrolyte (Table 1).

Take the prepared V(V) electrolyte as the pristine, 16g electrolyte sample was added to the glass tube with plug, then added additive to the electrolyte according to the proportion of 0.5 wt%, shake well, that was the mixed electrolyte used as experiments.

2.2 Study on the stability of V(V) electrolyte

The temperature has a great influence on the stability of V(V) electrolyte, and V₂O₅ precipitates easily from the positive electrolyte at high temperature, which affects the performance of the battery. Generally, it can keep the whole vanadium electrolyte system in a stable temperature range of 10~40 °C, and the higher the concentration of vanadium ions, the more difficult it is to maintain stability. The stability of mixed electrolyte with different additives was studied in a wide temperature range of -5~45 °C. The prepared stopper tube containing mixed electrolyte was sealed and placed in a constant temperature device under different temperature conditions. Maintain the static state for 30 days under the set temperature, observe the state change of electrolyte in the test tube with naked eyes at a fixed time interval, and record the generation process of red precipitate of V₂O₅ brick (the time interval at the initial stage of experiment could be appropriately shortened, and the observation time interval at high temperature should be short). After 30 days of investigation, the supernatant in the tube was removed to determine the concentration of V(V) ions.

2.3 Study and characterization of electrochemical properties of positive electrolyte

2.3.1 Cyclic voltammetry (CV)

The instrument and model used for CV tests were Shanghai Chenhua CHI-600 C electrochemical workstation, the temperature was 25 °C, and the three-electrode system was used for determination. The preparation method of the mixed electrolyte with an additive to be investigated was as described above, and the mixing ratio was 0.5 wt%. The range of measurement was 0~1 V, and the sweep rate was 0.01~0.1 V/s.

2.3.2 Polarization curve

The steady-state polarization experiments can be used to study the charge transfer dynamics of the active substances on the electrode surface, and the results can also be used to further verify the CV. The steady-state polarization experiment was carried out at room temperature on the Autolab 302 electrochemical workstation, using the same three-electrode test system as the cyclic voltammetry, with the open circuit potential as the midpoint and the scanning rate of 1 mV/s.

2.3.3 High temperature concentration curve

As the precipitation process and concentration variation of V(V) electrolyte were slow at 45 °C, the temperature for observation increased to 60 °C, and the concentration change curve of V(V) ions with time has been obtained.

2.3.4 UV-vis and Raman spectrum measurement of V(V) electrolyte

UV-vis spectrum is a method to determine the absorbance of substances in the wavelength range of 190-800nm, which is used for identification, impurity inspection and quantitative determination. The change of V(V) ions in the solution after adding additives was measured by UV-vis spectrophotometer (UN-1780) in the range of 200-900nm (investigated after 30 times dilution of electrolyte). Raman spectrum (Finder Vista) experiment was carried out on the electrolyte samples at room temperature to observe the variation in the chemical bonds in the electrolyte system after adding the high-quality additive.

2.3.5 Battery performance

1.8 M V(IV) + 3.0 M H₂SO₄ was selected as the initial positive electrolyte. A certain amount of additive was added to the positive electrolyte with a specific proportion before experiment until it was completely dissolved. 1.8 M V(IV) + 3.0 M H₂SO₄ was the initial negative electrolyte. The constant current charge and discharge experiment was carried out on a battery tester (CT2001A-5V/2A) at room temperature. The upper voltage limit was set to 1.6 V and the lower limit to 0.8 V. The cycle charge and discharge curves at 60 mA/cm² were obtained respectively.

2.3.6 SEM, EDS and XPS

SEM (FEI Inspect F50) and EDX (EDAX super octane) was carried out on the graphite felt with 100 cycles of cyclic charge discharge experiment. The content of elements on the graphite felt was obtained at the same time and the results were further verified by XPS (AXIS Ultra DLD).

3. RESULTS AND DISCUSSION

3.1 Effect of additives on the stability of positive electrolyte

Table 2. Thermal stability results of V(V) electrolyte with organic carboxylic potassium salts additives

Additive (0.5 w%)	Precipitation time			
	-5°C	25°C	45°C	60°C
Pristine	30 D	30 D	20 h	2.5 h
KAc	30 D	30 D	8 h	1 h
KDF	30 D	30 D	30 h	3 h
KAH	30 D	30 D	20 h	2 h

The stability of the mixed electrolyte sample with additives had been experimented and analyzed at different temperatures. Table 2 showed the thermal stability experimental data of V(V) electrolyte with the organic carboxylic potassium salts additives. KDF (in acid solution, it could be regarded as containing carboxyl group) with hydroxyl or carboxylic group could be used as good additives to improve the stability of electrolyte, for the reasons similar to those mentioned above, that was to say, the primary hydroxyl was easy to be oxidized by VO_2^+ ions and part of VO_2^+ ions were reduced to VO^{2+} ions, which changed the composition of the electrolyte, from the original V(V) solution to the V(V)/V(IV) electrolyte containing a small amount of VO^{2+} ions, which is equivalent to reducing the concentration of VO_2^+ ions and improves the stability accordingly. Or because large number of hydroxyl groups in these additive molecules would be adsorbed on the surface of VO_2^+ hydrated ions, the coulomb electrostatic repulsion effect and steric resistance effect would make VO_2^+ hydrated ions more dispersed[25], hinder the conversion of V(V) ions to V_2O_5 precipitation, and improved the stability of electrolyte.

3.2 Electrochemical performance

The results of the thermal stability experiment represent that KDF could inhibit precipitation at high temperature. To further verify the effect of these additives, the electrochemical performance of the mixed electrolyte was investigated. The electrochemical behavior of the mixed electrolyte was measured by cyclic voltammetry, and the relevant parameters such as electrochemical activity and reversibility were obtained.

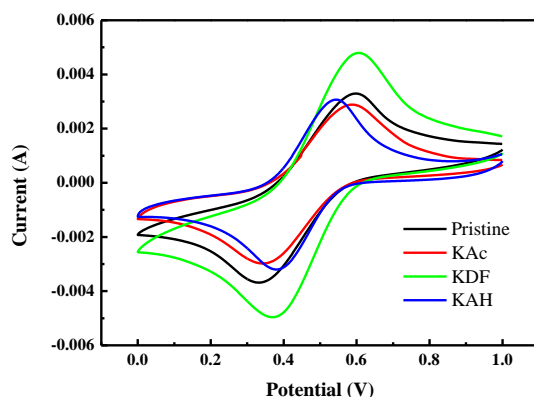


Figure 1. CV curves of different electrolyte samples (25°C, scanning rate: 0.05V/s)

Table 3. CV data of different electrolyte samples (25°C, scanning rate: 0.05V/s)

Additive	Oxidation peak		Reduction peak		ΔV	I_O/I_R
	Voltage/V	Current/A	Voltage/V	Current/A		
Pristine	0.597	0.00329	0.332	-0.00368	0.265	0.89402
KAc	0.588	0.00328	0.343	-0.00298	0.245	1.10067
KDF	0.606	0.00479	0.37	-0.00496	0.236	0.96654
KAH	0.544	0.00285	0.38	-0.00336	0.164	0.84821

The results of CV on electrolyte samples were shown in Fig.1. It could be observed that the CV curves of different samples with similar shapes and same peak shape. Due to the addition of KDF, the peak position and current intensity of V(IV)/V(V) redox peak were different. The corresponding results were listed according to their electrochemical data. It could be seen from Table 3 that KDF had a significant enhancement effect on the electrochemical activity of V(V) positive electrolyte (I_o increased by 45.6%), and the electrochemical reversibility was also improved.

3.3 Analysis of ion diffusion process

CV data showed that the addition of KDF improved the electrochemical activity and reversibility of the V(V) electrolyte. From the CV data of different scanning rates, we could also compare the changes in the ion diffusion process of the electrolyte. Theoretically, the diffusion coefficient (D) of quasi reversible reaction is between that of reversible reaction and irreversible reaction (D_1 and D_2)[25]. The conversion of V(V) ions to V(IV) ions on the electrode surface can be regarded as a quasi reversible reaction process, and it is a single step sudden single electron reaction[26].

For the reversible reaction of one step and one electron, peak current intensity i_p (mA) can be expressed as Eq. (5): $i_p = 0.4463 (F^3/RT)^{1/2} ACD_1^{1/2} v^{1/2}$ (5)

For the irreversible reaction of the single step and a single electron, the expression of i_p (mA) is Eq. (6): $i_p = 0.4958 (F^3/RT)^{1/2} \alpha^{1/2} ACD_2^{1/2} v^{1/2}$ (6)

Where, F is Faraday constant (96485 C/mol), R is a general gas constant (8.314 J/mol·K), T is experiment environment temperature (K), A is working electrode surface area (cm^2), C is active substance concentration (M), D_1 and D_2 are the diffusion coefficients ($\text{cm}^2 \cdot \text{s}^{-1}$), v is the scanning velocity (V/s), and α is the transfer coefficient (0.5 for a single step and one electron reaction).

The experiments in this section were carried out at room temperature (25 °C), $T = 25^\circ\text{C} = 298.15\text{ K}$; the diameter of the working electrode was 2 mm, the electrode area was 0.0314 cm^2 ; the concentration of V(V) electrolyte used in this experiment was 2.876 M. According to these existing constant values and known values, substituting them into the expression of i_p , we could deduce Eq. (7), (8):

$$\text{Reversible reaction: } i_p = 24.29 D_1^{1/2} v^{1/2} = kv^{1/2} \quad (7)$$

$$\text{Irreversible reaction: } i_p = 27.00 D_2^{1/2} v^{1/2} = kv^{1/2} \quad (8)$$

Therefore, the peak current intensity i_p was linearly related to the square root $v^{1/2}$ of scanning rate, and the slope is k . i_p was used to express the diffusion coefficient D, including:

$$D_1 = 1.69 \times 10^{-3} k^2 ; D_2 = 1.37 \times 10^{-3} k^2$$

It could be seen from the expressions of D_1 and D_2 that the diffusion coefficient was only related to the slope k of the line formed by the peak current intensity (i_p) and the square root of scanning rate ($v^{1/2}$), and the diffusion coefficient D increased with the increase of slope k . For the quasi reversible reaction, the diffusion coefficient D lay between D_1 and D_2 , and there was no accurate expression. Only the values of D_1 and D_2 could show the approximate range, which provided a reference data basis for the ion diffusion kinetics of the quasi reversible reaction.

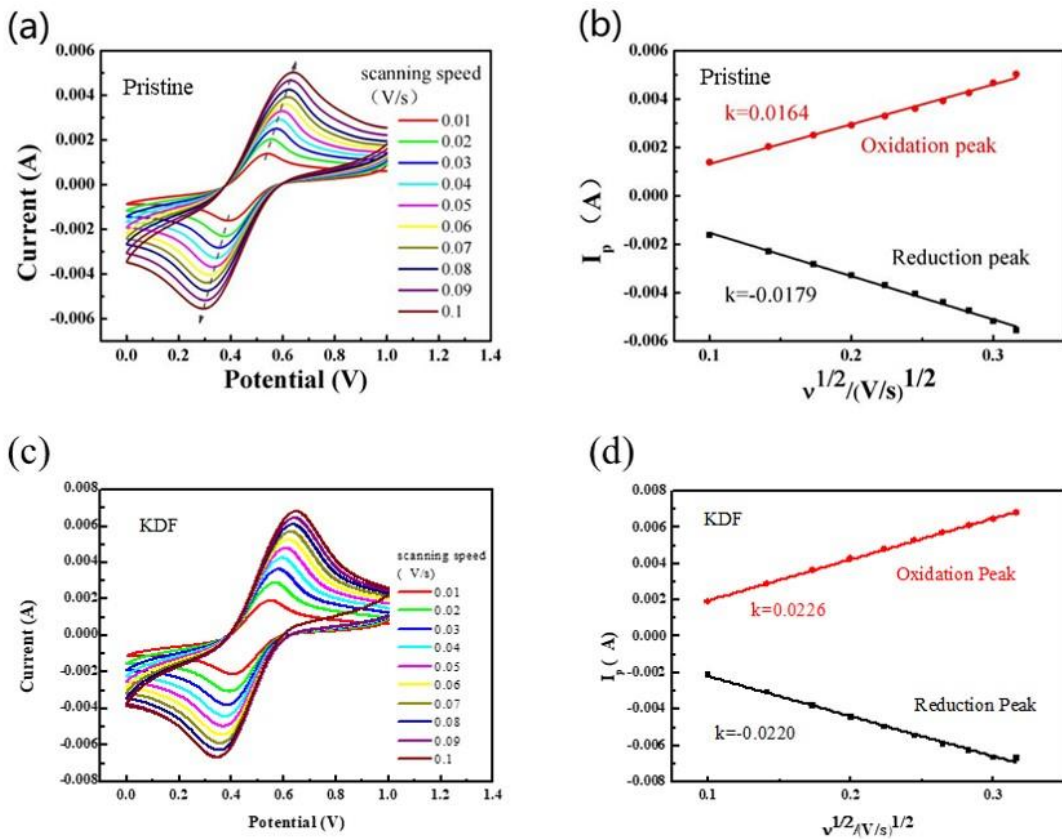


Figure 2. (a) CV curves of different scanning rates on a graphite electrode at 25 °C for the pristine; (b) correlation between I_p and $v^{1/2}$ at different scanning rates; (c) CV curves of different scanning rates on a graphite electrode at 25 °C for the KDF; (d) correlation between I_p and $v^{1/2}$ at different scanning rates

Take the pristine as an example, and the CV curves at different scanning rates were shown in Fig.2(a). It could be found that the redox peak current intensity i_p gradually increased with the increase of scanning rate. Due to the influence of solution and wire resistance, the redox peak potential difference slightly increased at different scanning rates, but the overall change was small, the maximum difference was about 100 mV, and the reversibility was excellent. These data showed that the redox process of V(V)/V(IV) electric pair was a quasi reversible process. According to the relation of sweep rate of peak current intensity in Fig.2(a), the corresponding $i_p-v^{1/2}$ curves were got (Fig.2(b)). $i_p-v^{1/2}$ had obvious linear relation. The fitting curve was obtained, and the slope k was used to express the values of D_1 and D_2 . According to the slope of the fitting curve, the oxidation process was $k= 0.0164$; the reduction process was $k= -0.0179$. According to the obtained results, at 25 °C, $D_1= 1.69\times 10^{-3}k^2$; $D_2= 1.37\times 10^{-3}k^2$, the oxidation process $D_1= 4.55\times 10^{-7}$; $D_2= 3.68\times 10^{-7}$; the reduction process $D_1= 5.41\times 10^{-7}$; $D_2= 4.39\times 10^{-7}$.

Generally, the oxidation peak current intensity was selected as the peak current intensity for data comparison. The mixed electrolyte sample after adding KDF was investigated and analyzed under the same condition.

Table 4. Ion diffusion coefficients of different electrolyte samples at 25°C

Additive	Slope (k)	D_1 ($\times 10^{-7}$)	D_2 ($\times 10^{-7}$)
Pristine	0.0164	4.55	3.68
KDF	0.0226	8.62	6.99

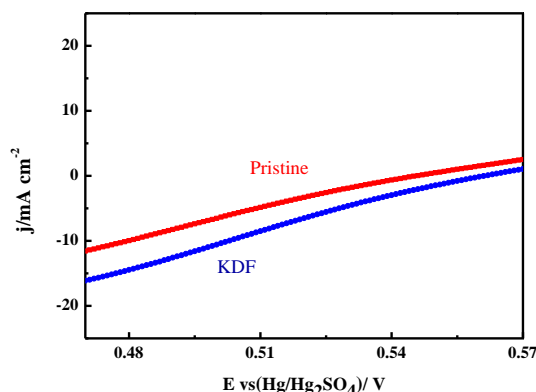
Table 4 summarized the diffusion coefficient of V(V) ions of different electrolyte samples. From the values of the diffusion coefficients D_1 and D_2 , it could be found that, compared with the pristine, the diffusion coefficient of the pristine electrolyte was significantly increased after adding KDF, the diffusion process of V(V) ions was accelerated, and the reaction process of V(V)/V(IV) electric pair on the electrode surface was accelerated.

3.4 Polarization curve analysis

In addition to further study of ion diffusion process, the method of charge transfer dynamics could also be demonstrated by the steady-state polarization experiment. In this section, the steady-state polarization experiment with a scanning rate of 0.001V/s was carried out on V(V) electrolyte samples. The kinetic constants of the electrode reaction of V(V)/V(IV) redox pair on the graphite electrode surface at 25 °C were analyzed and explored. When the overpotential i is low, there is a linear relationship between the current intensity I (mA/cm²) and the overpotential η (V)[7,9]. Therefore, the slope of the i - η curve is the polarization resistance R_p (Ω·cm²). Through R_p , the exchange current density i_0 (mA/cm²) can be further calculated, and then the reaction standard rate constant k_0 (cm/s) can be obtained. The transformation relations between these values are Eq. (9):

$$R_p = \frac{\eta}{i_0}, \quad i_0 = \frac{RT}{nFR_p}, \quad k_0 = \frac{i_0}{nFC_0} \quad (9)$$

Among them, n is the number of charge transfer, n value is 1 in the V(V)/V(IV) ion conversion process; F is Faraday constant (96485 C/mol); R is a general gas constant (8.314 J/mol · K); T is the experiment environment temperature (298.15 K); C_0 is the concentration of the active substance (M), and the concentration of vanadium ions in the electrolyte used in this experiment is 2.876 M.

**Figure 3.** Steady-state polarization curve of different electrolyte samples at 25 °C with a scanning rate of 1 mV/s

The results of the steady-state polarization experiment on different samples under the same conditions were shown in Fig.3. At 25 °C, compared with the pristine, the polarization resistance changed after adding KDF.

Table 5. Kinetic parameters of different electrolyte samples

Additive	R_p (Ωcm^2)	i_0 (mAcm^{-2})	k_0 (10^{-5}cms^{-1})
Pristine	7.21281	3.56189	1.28361
KDF	6.12153	4.19687	1.51243

In order to obtain the accurate change of polarization resistance, the curve was fitted to obtain the corresponding electrochemical data. From Table 5, it could be seen that after adding KDF, the polarization resistance of the solution decreased to $6.12 \Omega\cdot\text{cm}^2$, the corresponding exchange current density increased to $4.20 \text{ mA}/\text{cm}^2$, and the corresponding standard rate constant increased by 1.51 cm/s , which accelerated the redox reaction kinetics of V(V)/V(IV) pair in the electrolyte.

3.5 Concentration curve

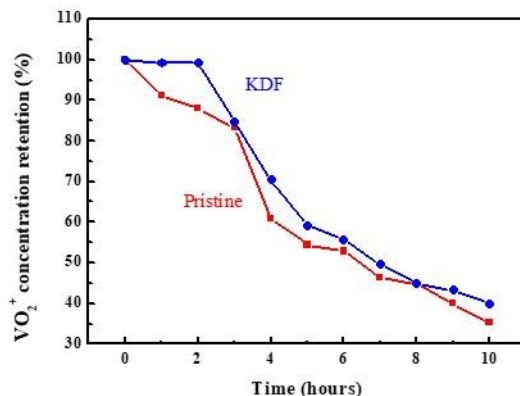


Figure 4. Concentration change curves of VO_2^+ ions at 60 °C (initial concentration: 2.876 M)

The electrochemical activity and kinetic parameters of V(V) indicated the superiority of KDF. In order to explore the performance of its practical application, it was necessary to observe the concentration change at high temperature. At 60 °C, V(V) and V(V) + KDF were investigated at static high temperature. The change of solution state and V(V) ions concentration were observed every hour. 10 hours later, the two electrolyte samples were precipitated completely. The change curves of concentration were as shown in Fig.4. It could be seen that after adding KDF, the anode electrolyte could maintain a long time stability at 60 °C, and the concentration of V(V) ions was as high as 99.2% of initial concentration after two hours, and the precipitation phenomenon was obvious only when the time continues to be extended (obvious precipitation appeared after about 3h), while the V(V) ions without

additives were unstable at 60 °C, and could maintain a stable state after one hour, and the maintenance rate of V(V) ions decreased obviously, and the maintenance rate was only 88%. In the follow-up process, the VO_2^+ maintenance rate of KDF sample was higher than that of the pristine one. 10 hours later, the VO_2^+ maintenance rate of the sample added with KDF was 40%, while the pristine was 35.2%. The results showed that the addition of KDF could effectively inhibit the irreversible V_2O_5 precipitation process and prolong the stability time of the electrolyte at high temperature.

3.6 UV-vis and Raman spectrum

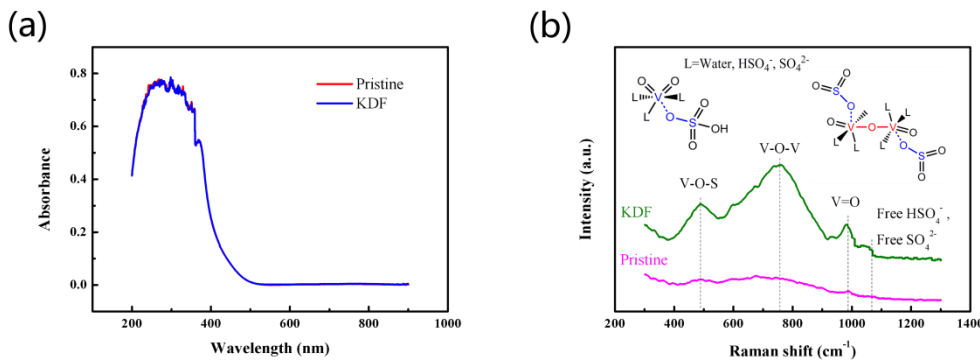


Figure 5. (a) UV-vis and (b) Raman spectra and corresponding characteristic peaks of pristine and mixed additive samples

According to the above results, it had been found that KDF could inhibit precipitation of V(V) electrolyte at high temperature. To explore the mechanism of inhibiting precipitation, the electrolyte was tested by UV-vis and Raman spectroscopy (Fig.5). The broad absorption peak of V(V) ions could be observed at 300 nm by UV-vis spectrum, and the peak shape was unchanged after KDF addition (Fig.5(a)), which showed that the state of V(V) ions in the electrolyte was not affected, and the ion concentration and valence state were unchanged. That was to say, KDF could be used as a stable V(V) electrolyte additive. The Raman contrast between the pristine and the mixed sample was shown in Fig.5(b). It could be seen that after adding KDF, the mixed electrolyte had obvious characteristic peak, and the strongest V-O-V characteristic peak (in the form of $\text{V}_2\text{O}_3^{4+}$ dimer[11] oxygen bridging) appeared in the range of 720-800 cm^{-1} . Secondly, V-O-S characteristic peak appeared in the range of 430-480 cm^{-1} due to the absorbing of SO_4^{2-} , V=O characteristic peak appeared in the range of 980-1020 cm^{-1} , and weak free HSO_4^- and SO_4^{2-} appeared in the range of 1030-1100 cm^{-1} [26]. The results showed that the addition of KDF promoted the formation of $\text{V}_2\text{O}_3^{4+}$ dimer oxygen bridging, and the formation of a large number of dimer ions was conducive to the stability of the V(V) electrolyte system, which may be the reason for the significant improvement of the electrochemical performance and high-temperature stability of the electrolyte system with KDF.

3.7 Battery performance

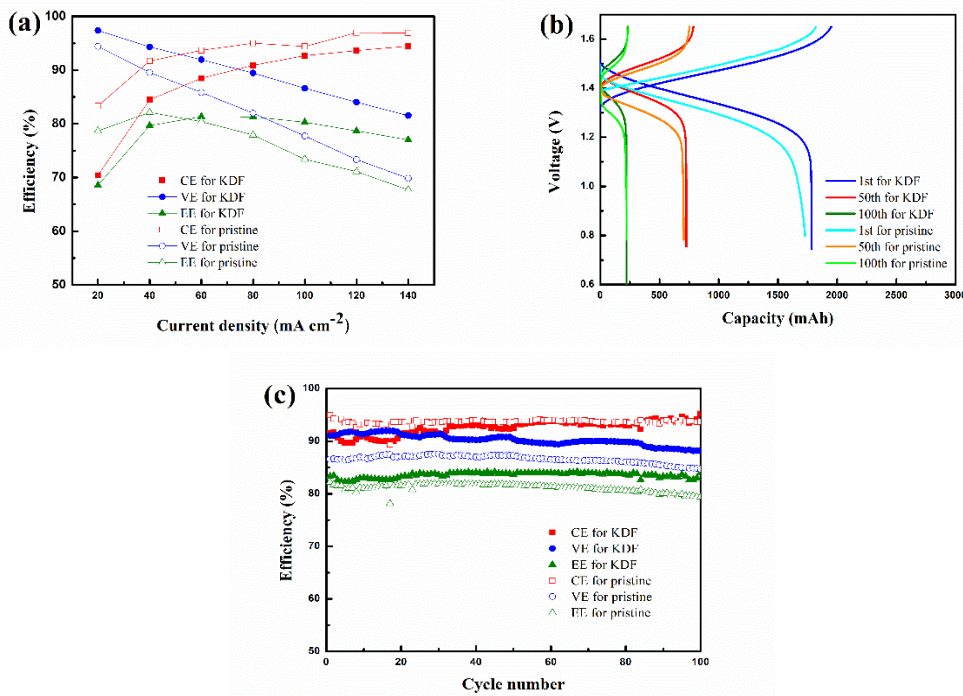


Figure 6. Comparison of (a) efficiency curves from 20 to 140 $\text{mA} \cdot \text{cm}^{-2}$, (b) cycle charge and discharge curves and (c) efficiency curves of cycle charge and discharge at 60 $\text{mA} \cdot \text{cm}^{-2}$ for VRFB with the pristine and KDF (EE: energy efficiency; CE: coulomb efficiency; VE: voltage efficiency).

In order to verify the practical application effect of the KDF additive, the charge and discharge tests of the single battery with V(V) electrolyte containing KDF were performed. The charge-discharge performance of the pristine and KDF samples was carried out from 20 to 140 $\text{mA} \cdot \text{cm}^{-2}$. As shown in Fig.6(a), the CE of battery with the pristine and KDF exhibited a clear upward trend with the rise of current density, while the VE decreased linearly, the coaction of CE and VE resulted in an increase at first in EE and then a decrease. It was observed that the EE of battery with KDF reached the maximum at 60 $\text{mA} \cdot \text{cm}^{-2}$, so the current density was used for further cycle charge -discharge investigation. Fig.6(b) showed the cycle charge and discharge curves of the 1st, 50th, and 100th cycles. The addition of KDF could clearly increase the charge-discharge capacity and improved the discharge platform although the positive effect slightly diminished as the number of cycles increases that might be due to the oxidation of $-\text{COO}^-$ in the KDF. It could be seen from Fig.6(c), KDF could significantly improve the VE, which was consistent with the results of CV and polarization. The EE (average 83%) was higher and more stable compared with the pristine (average 81%), yet CE fluctuated seriously and the overall trend was upward, while VE fluctuated slightly and the overall trend was downward during cycling, which might be attributed to the oxidation of $-\text{COO}^-$ and release of CO_2 . Overall, the addition of KDF in V(V) electrolyte could improve the cycling performance of the battery and KDF was proved to be a candidate additive for V(V) electrolyte.

3.8 SEM, EDS and XPS

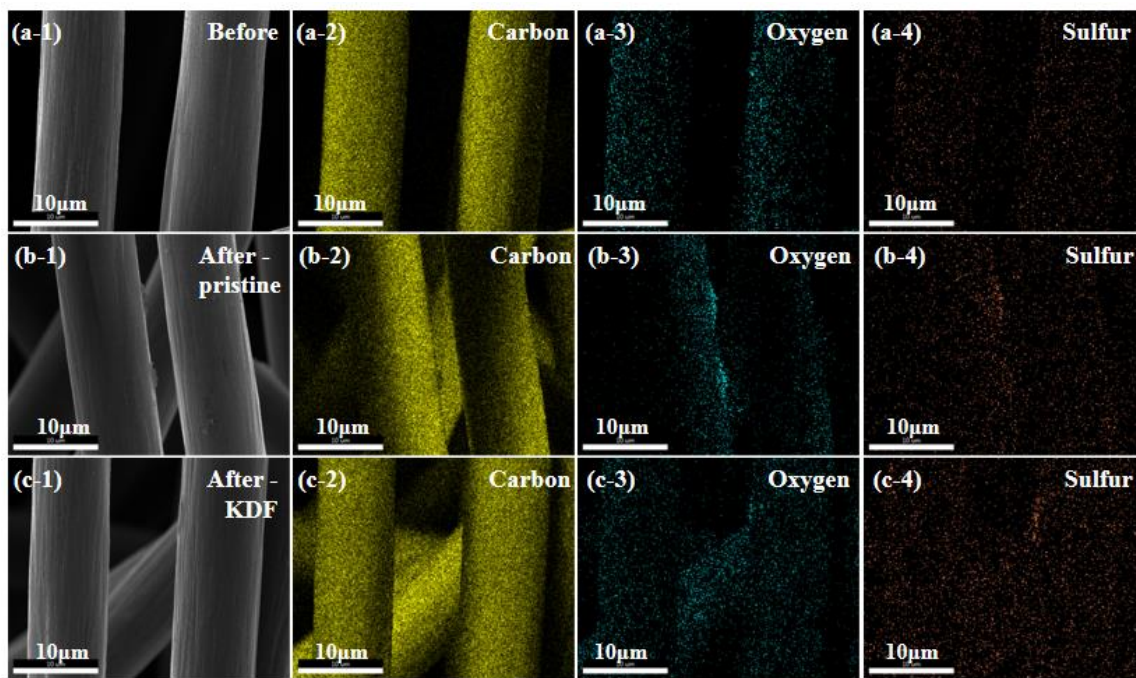


Figure 7. Comparison of surface morphology and element distribution (C, O, S) of graphite felt (a) before, (b) after-pristine and (c) after- KDF cyclic experiment

Table 6. Surface element distribution of graphite felt before and after cyclic experiment

	Wt/%			Atomic percentage/%		
	C	O	S	C	O	S
Before	97.92	1.25	0.19	98.7	0.95	0.07
After-pristine	97.22	1.81	0.29	98.24	1.38	0.11
After- KDF	97.06	1.90	0.35	98.12	1.44	0.13

In order to explore the mechanism of improving the performance of V(V) electrolyte by KDF, SEM and EDX were carried out on the positive graphite felt electrode in the battery after 100 cycles tests and the corresponding morphology and element distribution of the graphite felt surface were obtained. It was observed that the surface morphologies of graphite fiber in graphite felt electrode after treatment in different condition changed a little (Fig.7). Nevertheless, for the samples with KDF and the pristine, the content of O, S increased while the content of C decreased after cycling (Table 6). And the content change of C, O, S for the sample with KDF was much greater, that might be ascribed to the adhesion of KDF on the surface of the graphite felt increasing the content of C=O and $V_2O_3^{4+}$ dimer structures [11, 27] due to the etching of the electrode surface and adsorbing of SO_4^{2-} , which promoted

the redox reaction process and the contact effect between electrode with the electrolyte, thus improving the overall performance of the battery.

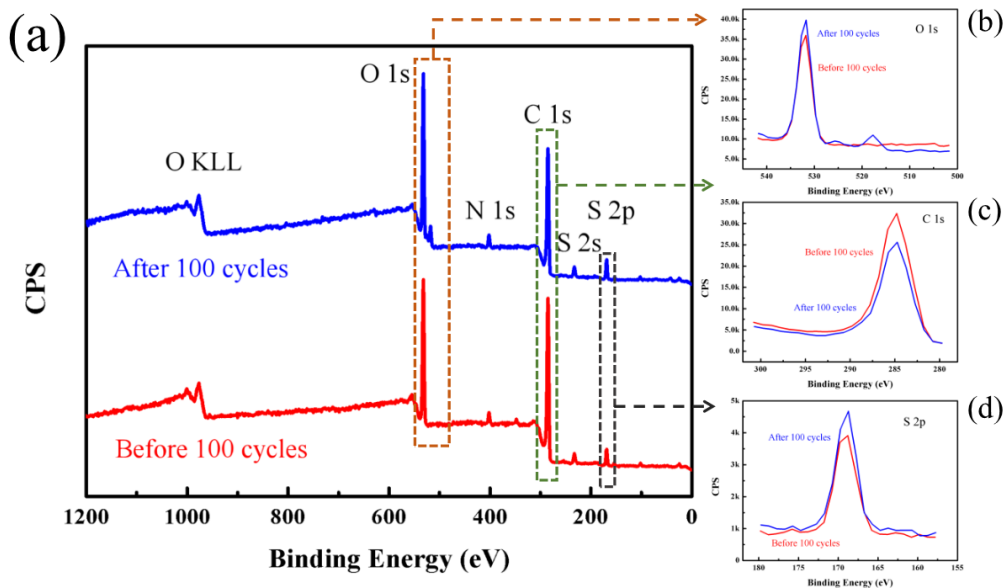


Figure 8. XPS spectra of the graphite felt electrode. (a) XPS spectra of graphite felt surface before and after 100 cycles experiment and (b) O 1s (c) C 1s and (d) S 2p spectra of carbon felt

Moreover, the content of C, O, S on the graphite felt electrode after 100 cycling tests were further verified by XPS. As shown in Fig.8, it could be seen that after the cyclic experiment, the content of O and S elements on the surface of graphite felt increased, the signal of O element increased by 10.6%, and the signal of S element increased by 19.6% as soon as C decreased by 20.9%, which agreed with the results of EDS.

3.10 Performance comparison

Table 7. Performance comparison of different additives

Additive	Concentration of V(V)	Time of precipitation formation	Energy efficiency	Reference
KDF	2.876 M	20h (45°C) ; 2 h (60°C)	83% (100 cycles)	This work
Sodium formate	1.8 M	16.52h (50°C) ; 2.75 h (60°C)	79.0% (50 cycles)	[24]
Taurine	1.5 M	2 h (40°C)	87.9% (100 cycles)	[28]

Combined with relevant literature [24, 28], the performance of KDF was compared with that of the same type of additives, and the data was shown in Table 7. The results showed that KDF still had

comparable thermal stability and battery performance in a high concentration V(V) electrolyte system, indicating that KDF is a promising additive for VRFB positive electrolyte.

4. CONCLUSION

Through the study of three organic carboxylic potassium salt as additives of V(V) electrolyte, KDF was an additive that had significantly improved in thermal stability, electrochemical activity, and reversibility, ion diffusion effect, battery performance, etc. The addition of KDF promoted the formation of $V_2O_3^{4+}$ dimer oxygen bridge structure in V(V) electrolyte system and effectively inhibited the formation of V_2O_5 precipitation. This result promoted the stability of the electrolyte system at high temperature. Compared with the pristine, the V(V) electrolyte with KDF was more stability at 45 °C and 60 °C. The maintenance of VO_2^+ concentration in V(V) electrolyte with KDF for 2 hours at 60 °C was 99.2%, which was much higher than that of V(V) electrolyte without KDF (88%, obvious precipitation appeared after 3h). After 100 cycles, the energy efficiency of V(V) sample with KDF (average 83%), which was significantly better than the pristine (average 81%). The addition of KDF effectively enhanced the activity of graphite felt, thus improving the performance of electrolyte and the overall performance of battery. All the results showed that KDF could be used as an additive for high-quality VRFB positive electrolyte.

ACKNOWLEDGMENT

This work was supported by the National Natural Science Foundation of China (51602209) and the Fundamental Research Funds for the Central Universities (2018SCUH0025).

NOTES

The authors declare no competing financial interest.

References

1. M. Skyllas-Kazacos, M. Rychcik, R.G. Robins, A.G. Fane and M.A. Green, *J. Electrochem. Soc.*, 133 (1986) 1057.
2. C. Fabjan, J. Garche, B. Harrer, L. Jorissen, C. Kolbeck, F. Philippi, G. Tomazic and F. Wagner, *Electrochim. Acta*, 47 (2001) 825.
3. L. Joerissen, J. Garche, C. Fabjan and G. Tomazic, *J. Power Sources*, 127 (2004) 98.
4. M. Skyllas-Kazacos, M.H. Chakrabarti, S.A. Hajimolana, F.S. Mjalli and M. Saleem, *J. Electrochem. Soc.*, 158 (2011) R55.
5. M. Skyllas-Kazacos, C. Peng and M. Cheng, *Electrochem. Solid-State Lett.*, 2 (1999) 121.
6. T.D. Nguyen, L.P. Wang, A. Whitehead, N. Wai, G.G. Scherer and Z.J. Xu, *J. Power Sources*, 402 (2018) 75.
7. G. Wang, J. Chen, X. Wang, J. Tian, H. Kang, X. Zhu, Y. Zhang, X. Liu and R. Wang, *J. Electroanal. Chem.*, 709 (2013) 31.
8. M. Vijayakumar, L.Y. Li, G. Graff, J. Liu, H.M. Zhang, Z.G. Yang and J.A. Hu, *J. Power Sources*, 196 (2011) 3669.
9. G. Wang, J. Chen, X. Wang, J. Tian, H. Kang, X. Zhu, Y. Zhang, X. Liu and R. Wang, *J. Energy*

- Chem.*, 23 (2014) 73.
- 10. J. Zhang, L. Li, Z. Nie, B. Chen, M. Vijayakumar, S. Kim, W. Wang, B. Schwenzer, J. Liu and Z. Yang, *J. Appl. Electrochem.*, 41 (2011) 1215.
 - 11. N.V. Roznyatovskaya, V.A. Roznyatovsky, C.-C. Hoehne, M. Fuehl, T. Gerber, M. Kuettinger, J. Noack, P. Fischer, K. Pinkwart and J. Tuebke, *J. Power Sources*, 363 (2017) 234.
 - 12. S. Roe, C. Menictas and M. Skyllas-Kazacos, *J. Electrochem. Soc.*, 163 (2016) A5023.
 - 13. C. Ding, X. Ni, X. Li, X. Xi, X. Han, X. Bao and H. Zhang, *Electrochim. Acta*, 164 (2015) 307.
 - 14. F. Rahman and M. Skyllas-Kazacos, *J. Power Sources*, 340 (2017) 139.
 - 15. N. Kausar, A. Mousa and M. Skyllas-Kazacos, *Chemelectrochem*, 3 (2016) 276-282.
 - 16. S.-K. Park, J. Shim, J.H. Yang, C.-S. Jin, B.S. Lee, Y.-S. Lee, K.-H. Shin and J.-D. Jeon, *Electrochim. Acta*, 121 (2014) 321.
 - 17. L.Y. Li, S. Kim, W. Wang, M. Vijayakumar, Z.M. Nie, B.W. Chen, J.L. Zhang, G.G. Xia, J.Z. Hu, G. Graff, J. Liu and Z.G. Yang, *Adv. Energy. Mater.*, 1 (2011) 394.
 - 18. Z. Jia, B. Wang, S. Song and X. Chen, *J. Electrochem. Soc.*, 159 (2012) A843.
 - 19. C.S. Jin, J.Y. So, K.H. Shin, E.B. Ha, M.J. Choi, S.K. Park, Y.J. Lee and S.H. Yeon, *J. Appl. Electrochem.*, 48 (2018) 1019.
 - 20. F. Chang, C. Hu, X. Liu, L. Liu and J. Zhang, *Electrochim. Acta*, 60 (2012) 334.
 - 21. L. Cao, M. Skyllas-Kazacos, C. Menictas and J. Noack, *J. Energy Chem.*, 27 (2018) 1269.
 - 22. X.W. Wu, S.Q. Liu and K.L. Huang, *J. Inorg. Mater.*, 25 (2010) 641.
 - 23. S. Abbas, J. Hwang, H. Kim, S.A. Chae and H.Y. Ha, *ACS Appl. Mater. Inter.*, 11 (2019) 30.
 - 24. D. Kim, J. Jeon, *Journal Of Electroanalytical Chemistry* 801 (2017) 92.
 - 25. Q. Liu, A.A. Shinkle, Y. Li, C.W. Monroe, L.T. Thompson and A.E.S. Sleightholme, *Electrochem. Commun.*, 12 (2010) 1634.
 - 26. S. Zhong and M. Skyllas-Kazacos, *J. Power Sources*. 39 (1992) 1.
 - 27. Y.D. Yang, Y.M. Zhang, T. Liu and J. Huang, *Res. Chem. Intermediat.*, 44 (2018) 769.
 - 28. J. Hwang, B.M. Kim, J. Moon, A. Mehmood and H.Y. Ha, *J. Mater. Chem. A*, 6 (2018) 4695.